University of Anbar

Anbar Journal Of Engineering Science©

journal homepage: http:// http://www.uoanbar.edu.iq/Evaluate/

Effect of Grooves Geometric Parameters on Hydraulic Thermal Performance of Circular Pipe Partially Filled with Metallic Foam

Obaid T. Fadhil, Hamdi E. Ahmed, Wisam A. Salih

Department of Mechanical Engineering, College of Engineering, University of Anbar Ramadi, Iraq

PAPER INFO

Paper history:
Received … … …
Received in revised form … … …
Accepted … … …

Keywords:
Hydraulic thermal design, enhancement metal foam, partially filled, pumping power,

ABSTRACT

The present paper addresses the numerical study of non-Darcy laminar forced convection flows in a pipe partially filled with grooved metallic foam attached in the inner pipe wall, which is subjected to a constant heat flux. Computations are carried out for nine different dimensions of grooves with different Reynolds numbers namely; ($250 \leq Re \leq 2000$) and their influences on the fluid flow and heat transfer are discussed. The governing and energy equations are solved using the finite volume method (FVM) with temperature-dependent water properties. The novelty of this work is developing of a new design for the metallic foam, which has not studied previously yet. It is observed that the two helical grooves with two pitches increase the *Nu* around 5.23% and decrease the pumping power nearly 12%. It is also showed a reduction in the amount of material required for manufacturing the heat exchanger, which leads to a decline in the weight of the system 8.29%.

1. INTRODUCTION

The metallic foam is a type of porous medium, the fluid flow and heat transfer in a pipe partially filled with metal foam are important in many engineering applications such as heat exchangers, chemical reactors, heat sinks, refrigeration, nuclear reactor cooling, etc. In order to improve design considerations for various applications, it is necessary to better understand the basic mechanisms in fluid flow and heat transfer. X. Chen et al. [1] studied numerically and analytically the Influence of using isotropic and homogeneous metallic foams in the heat exchangers. They introduced a performance factor to quantify the assessment of the compromise between heat transfer enhancement and pressure drop in designing a metal foam heat exchanger. V. V. Calmidi and R. L. Mahajan [2] studied experimentally and numerically a forced convection in high porosity of (aluminum, carbon, and copper foam). They showed that the effect of different parameters of aluminum foam (porosity, pores per inch (*PPI*), inertia coefficient, permeability) on Nusselt number and they found that the thermal dispersion can be very high and accounts for the bulk of the transport. M. Dehghan et al. [3] studied the influences of the different thermal conductivity of porous medium through the channel. They showed a linear rise in the thermal

conductivity of the medium effect in a semi-linear rise in the Nusselt number and they showed Nusselt number increases with Forchheimer number. M. Mahdavi et al. [4] studied numerically the heat transfer in a pipe partially filled with porous medium. They utilized variable values of porous thickness, layer position and permeability. They found that the increases in porous thickness and permeability led to increase the heat transfer when the porous medium placed in the inner wall. M. A. Teamah et al. [5] studied numerically the enhanced of heat transfer and pressure drop in the pipe partially filled with porous media. They have realized that the presence of porous media in the pipe significantly improves heat transfer. P. Taylor et al. [6] studied numerically the effect of inserted porous media partially filled in the pipe. They studied the effects of permeability, porous media thickness on the ΔP and *Nu*. They showed that *Nu* and ΔP increased with increasing the thickness of the porous media and the permeability. D. Poulikakos and M. Kazmierczak [7] studied theoretically the effect of thickness of the porous medium on the heat transfer enhancement in a channel partially filled with porous medium. They showed that Nu increased with increasing the thickness of porous medium. W. Lu et al. [8] presented an analytical study of the pipe that filled with metal foam. They showed that the pore size and the porosity of the metal foam playing an important role in the overall heat transfer rate. They also showed that the overall heat transfer rate increased with increasing the thermal conductivity of the metal foam. S. Mancin et al. [9] investigated the forced convection through foam samples with different porosities and *PPI*. They showed that the heat transfer increased with decreased *PPI*, and the pressure drops increased with increased *PPI*. V. V Calmidi and R. L. Mahajan [10] studied the influence of thermal conductivity of metal foams by experimental study with different porosities and *PPI*. They showed the effects of thermal conductivity increased with decreased the porosity at any number of PPI. Z. Qu et al. [11] studied the effect of the porosity on the *Nu* and ΔP in the pipe partially filled with metal foam. They showed that the increased in porosity led to decrease ΔP and led to increase in the *Nu* especially in ε=0.93. H.J. Xu et al. [12] studied the influence of *PPI* on the *Nu* and the *f* in the pipe that partially filled with metal. They showed that when *PPI* increased, *f* increased and *Nu* decreased. A.A. Sertkaya et al. [13] studied experimentally the effect of *PPI* with constant porosity on the pressure drop of the heat exchanger. They showed that the pressure drop was as low as possible in the 10 *PPI*, and the value of the pressure drop increased with increased *PPI*. C. Yang et al. [14] studied the influence of porous medium thickness on the Nusselt number in the pipe that partially filled with porous medium. They found the optimum value was recorded when porous medium were filled about 80% of the pipe to the full filled. Z. G. Qu and W. Q. Tao [15] studied the influence of the foam metals (copper, aluminum, nickel and stainless steel) on the *Nu*. They showed that a good value of the *Nu* in Copper and Aluminum, and *Nu* decreased in other metal. An addition of metallic foam to the pipe heat exchanger increases the heat removal with much increase in the pressure drop depending on the

value of the porosity and the *PPI*. Therefore, the need for enhancing the heat transfer and reducing the pumping power of fluids flow in pipes filled with porous media becomes principal in the designing of engineers. On the other hand, there are no study has been performed to seek the effect of grooved metallic foam on the hydrothermal performance of pipes partially filled.

2. Numerical simulation

2.1 Problem formulation

In this study, a horizontal pipe partially filled with grooved aluminum foam placed on the inner wall is studied. The diameter of the metal foam to the diameter of the pipe represents the value of the aspect ratio (*Ri*), which is equal to 0.55. The grooves are rectangular cross section. Therefore, several dimensions of the grooves were taken according to height (*H*) and width (*W*) that three values for height (6, 8, 10 mm) and three width values (3, 4, 5 mm), all dimensions experiment with each other. The grooves are controlled in straight (*SG*) and helical (*HG*) grooves as shown in **Figure 1**.

Table 1 Geometrical parameters.

H6	Height = 6mm	*W3*	Width =3mm
H8	Height =8mm	*W4*	Width =4mm
H10	Height =10mm	*W5*	Width =5mm
2SG	two straight grooves	*2HG*	two helical grooves

2.2 Assumptions

1. Flow is steady, Incompressible and laminar.
2. Convective liquid residues in a single-phase.
3. Aluminum foam is rigid, homogeneous, isotropic and saturated with liquid.
4. Local thermal equilibrium (*LTE*) ($T=T_s=T_f$).
5. Non- Darcy's law is valid i.e. inertial influences are significant.
6. The thermo-physical properties of the water are assumed to be variable with temperature.

2.3 Governing equations

The equations which describe the problem of forced convection in the pipe are mass, momentum, and energy [16],

Continuity Equation in cylindrical coordinates;

$$\frac{\partial}{\partial z}(\rho_f u)+\frac{1}{r}\frac{\partial}{\partial r}(\rho_f r v)+\frac{1}{r}\frac{\partial}{\partial \theta}(\rho_f w)=0 \quad (1)$$

Hollow region (without metal foam)

Momentum Equation *z*-component:

$$\rho_f\left(u\frac{\partial u}{\partial z}+v\frac{\partial u}{\partial r}+\frac{w}{r}\frac{\partial u}{\partial \theta}\right)=-\frac{\partial P}{\partial z}+\mu_f\left[\frac{\partial^2 u}{\partial z^2}+\frac{1}{r}\frac{\partial}{\partial r}\left(r\frac{\partial u}{\partial r}\right)+\frac{1}{r^2}\frac{\partial^2 u}{\partial \theta^2}\right] \quad (2)$$

r-component:

$$\rho_f\left(u\frac{\partial v}{\partial z}+v\frac{\partial v}{\partial r}-\frac{w^2}{r}+\frac{w}{r}\frac{\partial v}{\partial \theta}\right)=-\frac{\partial P}{\partial r}+\mu_f\left[\frac{\partial^2 v}{\partial z^2}+\frac{\partial}{\partial r}\left(\frac{1}{r}\frac{\partial r v}{\partial r}\right)+\frac{1}{r^2}\frac{\partial^2 v}{\partial \theta^2}-\frac{2}{r^2}\frac{\partial w}{\partial \theta}\right] \quad (3)$$

θ-component:

$$\rho_f\left(u\frac{\partial w}{\partial z}+v\frac{\partial w}{\partial r}+\frac{w}{r}\frac{\partial w}{\partial \theta}-\frac{vw}{r}\right)=-\frac{1}{r}\frac{\partial P}{\partial \theta}+\mu_f\left[\frac{\partial^2 w}{\partial z^2}+\frac{\partial}{\partial r}\left(\frac{1}{r}\frac{\partial r w}{\partial r}\right)+\frac{1}{r^2}\frac{\partial^2 w}{\partial^2 \theta}+\frac{2}{r^2}\frac{\partial v}{\partial \theta}\right] \quad (4)$$

Energy Equation

$$\left(\rho c_p\right)_f\left[u\frac{\partial T}{\partial z}+v\frac{\partial T}{\partial r}+\frac{w}{r}\frac{\partial T}{\partial \theta}\right]=k\left[\frac{\partial^2 T}{\partial z^2}+\frac{1}{r}\frac{\partial}{\partial r}\left(r\frac{\partial T}{\partial r}\right)+\frac{1}{r^2}\frac{\partial^2 T}{\partial \theta^2}\right] \quad (5)$$

Porous region

Momentum Equation [16]; z-component:

$$\frac{\rho_f}{\varepsilon^2}\left(u\frac{\partial u}{\partial z}+v\frac{\partial u}{\partial r}+\frac{w}{r}\frac{\partial u}{\partial \theta}\right)=-\frac{\partial P}{\partial z}+\frac{\mu_f}{\varepsilon}\left[\frac{\partial^2 u}{\partial z^2}+\frac{1}{r}\frac{\partial}{\partial r}\left(r\frac{\partial u}{\partial r}\right)+\frac{1}{r^2}\frac{\partial^2 u}{\partial \theta^2}\right]-\rho_f\frac{C_F}{K^{1/2}}u|U|-\frac{\mu_f}{K}u \quad (6)$$

r-component:

$$\frac{\rho_f}{\varepsilon^2}\left(u\frac{\partial v}{\partial z}+v\frac{\partial v}{\partial r}-\frac{w^2}{r}+\frac{w}{r}\frac{\partial v}{\partial \theta}\right)=-\frac{\partial P}{\partial r}+\frac{\mu_f}{\varepsilon}\left[\frac{\partial^2 v}{\partial z^2}+\frac{\partial}{\partial r}\left(\frac{1}{r}\frac{\partial r v}{\partial r}\right)+\frac{1}{r^2}\frac{\partial^2 v}{\partial \theta^2}-\frac{2}{r^2}\frac{\partial w}{\partial \theta}\right]- \quad (7)$$

$$\rho_f \frac{C_F}{K^{1/2}} v|U| - \frac{\mu_f}{K} v$$

θ-component:

$$\frac{\rho_f}{\varepsilon^2}\left(u\frac{\partial w}{\partial z} + v\frac{\partial w}{\partial r} - \frac{wv}{r} + \frac{w}{r}\frac{\partial w}{\partial \theta}\right) = -\frac{1}{r}\frac{\partial P}{\partial \theta} + \frac{\mu_f}{\varepsilon}\left[\frac{\partial^2 w}{\partial z^2} + \frac{\partial}{\partial r}\left(\frac{1}{r}\frac{\partial rw}{\partial r}\right) + \frac{1}{r^2}\frac{\partial^2 w}{\partial^2 \theta} - \frac{2}{r^2}\frac{\partial v}{\partial \theta}\right] - \rho_f \frac{C_F}{K^{1/2}} w|U| - \frac{\mu_f}{K} w \quad (8)$$

where $|U| = \sqrt{u^2 + v^2 + w^2}$ (9)

The Energy equation:

$$\left(\rho c_p\right)_f \left[u\frac{\partial T}{\partial z} + v\frac{\partial T}{\partial r} + \frac{w}{r}\frac{\partial T}{\partial \theta}\right] = k_e \left[\frac{\partial^2 T}{\partial z^2} + \frac{1}{r}\frac{\partial}{\partial r}\left(r\frac{\partial T}{\partial r}\right) + \frac{1}{r^2}\frac{\partial^2 T}{\partial \theta^2}\right] \quad (10)$$

In the above equation, $u, \boldsymbol{v}$ and w are the components of the velocity in z, r and θ directions, respectively, and T is the temperature and P is the pressure.

where k_e is the effective thermal conductivity [16][17]:

$$k_e = \varepsilon k_f + (1-\varepsilon) k_{aluminum\ foam} \quad (11)$$

$\mu_f = \mu_e$ [6]

2.4 Boundary conditions

At z = 0 (inlet) $v = w = 0$, $u = u_i$, $T = T_i$

At z = L (outlet)

$$\frac{\partial u}{\partial Z} = \frac{\partial v}{\partial Z} = \frac{\partial w}{\partial Z} = 0,\ p = p_{out} = 1\ atm,\quad \frac{\partial T}{\partial Z} = 0$$

(Thermally fully developed)

At $r = 0$, $\frac{\partial u}{\partial z} = v = w = 0$ $\frac{\partial T}{\partial z} = 0$

At $\theta = 0$, $\frac{\partial u}{\partial \theta} = \frac{\partial v}{\partial \theta} = \frac{\partial w}{\partial \theta} = 0$, $\frac{\partial T}{r\partial \theta} = 0$

At $\theta = \pi$, $\frac{\partial u}{\partial \theta} = \frac{\partial v}{\partial \theta} = \frac{\partial w}{\partial \theta} = 0$, $\frac{\partial T}{r\partial \theta} = 0$

The water temperature at the pipe inlet is taken as 300 K while the velocity is calculated based on the required Reynolds number ($250 \leq Re \leq 2000$). The thermo-physical properties of water and aluminum are adopted from **Ref. [18].**

Water	Aluminum	Aluminum Foam
Polynomial $\boldsymbol{Q = a + bT + cT^2}$	k=237 ($W\,m^{-1}\,K^{-1}$)	ε=0.93
	ρ=2702 ($kg\,m^{-3}$)	PPI=10
	c_p=903 ($J\,kg^{-1}\,K^{-1}$)	
	α=97.1e-6 ($m^2\,s^{-1}$)	

The thermo-physical properties of the water (i.e., density, viscosity, thermal conductivity, and specific heat) are taken as a temperature dependence in the numerical simulations in order to approximate the current *CFD* results to be enclosed to the experimental results [19]. The data of water properties is fitted according a polynomial equation as following

$$Q = a + bT + cT^2 \quad (12)$$

where Q represents any variable of water properties, a, b, and c are constant and T is the fluid temperature in Kelvin.

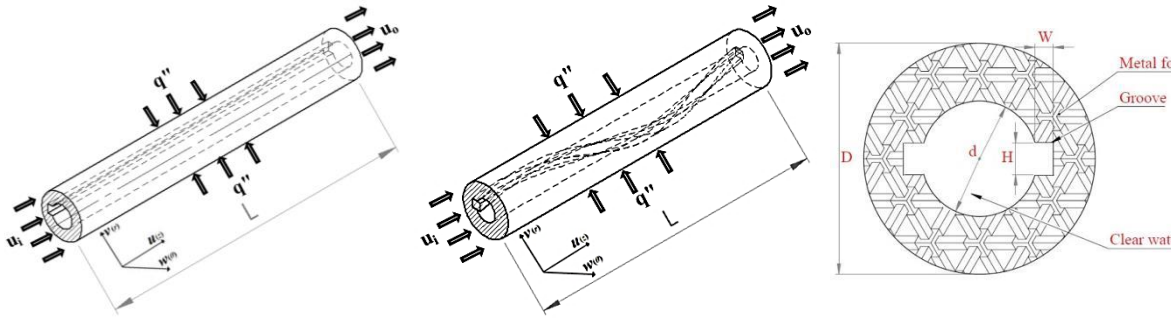

(a) (b) (c)

Figure 1. 3D Schematic diagram of the physical domain (a) straight groove, (b) helical groove and (c) Front side of the pipe.

2.5 Numerical calculations

The heat flux applied on the outer surface of the heated pipe is estimated by [18]:

$$q'' = -k_e \left.\frac{\partial T}{\partial r}\right|_{r=r_o} \quad (13)$$

The heat flux applied on the outer surface of the pipe equals the heat transferred by convection from the inner surface to the fluid, which is represented by the following equation:

$$q'' = h(T_w - T_b) \quad (14)$$

where T_w and T_b, the inner surface temperature and the water bulk temperature, respectively

$$h = \frac{q''}{(T_w - T_b)} \quad (15)$$

Hence, the local Nusselt number becomes

$$Nu_{\theta,Z} = \frac{h\,D}{k_e} = \frac{q''\,D}{k_e(T_w - T_b)} \quad (16)$$

The average Nusselt number is calculated by integrating equation (16) over the total surface of the heated wall as:

$$Nu = \frac{1}{A}\int_{Z=0}^{Z=L}\int_{\theta=0}^{\theta=2\pi} \mathrm{Nu}_{\theta,Z}\, r\, d\theta\, dZ \quad (17)$$

where A is the total convection area:

$$A = \pi DL \quad (18)$$

Then

$$Nu = \frac{hD}{k} \quad (19)$$

Reynolds number is defined according to the pipe diameter and the velocity of the fluid at the pipe inlet as:

$$Re = \frac{\rho_f . u_i . D}{\mu_f} \quad (20)$$

where *D* is the pipe diameter.

The friction factor through the pipe is calculated by

$$f = \frac{2D\Delta P}{L\,\rho_f u^2} \quad (21)$$

The performance evaluation criterion (*PEC*) is defined as

$$PEC = \frac{(Nu^*/Nu)}{(f^*/f)^{(1/3)}} \quad (22)$$

where *Nu** and *f** are the modified Nusselt number and modified friction factor (grooved metallic foam).

The pumping power can be calculated by:

$$PP = \dot{Q} \times \Delta P = u \times A_C \times \Delta P \ (Watt) \quad (23)$$

2.6 Numerical procedure

In order to analyze the fluid flow field and forced convection heat transfer in the pipe partially filled with metal foam, a solution of energy equation and Navier-stokes equations is required. Based on the conservation of mass, energy and momentum equations, the governing equations are obtained from these basic principles by applying them to a FVM, these are presented in Workbench built-in solver. The mathematical model of the constant and variable boundary conditions are solved numerically using a CFD Code FLUENT V.18.0 after describing the geometry using SolidWorks V.16.0.

It is necessary to have enough number of cells for a good resolution. The grid independence test is tested in order to find a fitting grid system. As shown in **Figure 2**, the deviations in the *Nu* and *f* results do not vary more than 0.03% and 0.14% respectively. At convergence, the discrete conservation equations (momentum, energy, etc.) are obeyed in all cells to a specified tolerance. Solution no longer changes with more iteration that can show in monitoring convergence with residuals. In the present work, the residuals used are the continuity, momentum and energy equation is about 1×10^{-6}.

2.7 Validation

The numerical computations are compared with the analytical solution of the cylindrical pipe partially filled with metal foam. Global Nusselt

number with all dimensionless radius of the metal foam radius to the pipe radius under the laminar flow is obtained by Xu et al. [12]. **Figure 3** shows the comparisons of the *Nu* and *Ri*. The current *CFD* results are in good agreement with the analytical solutions of [12], with maximum deviation of less than 7.5%.

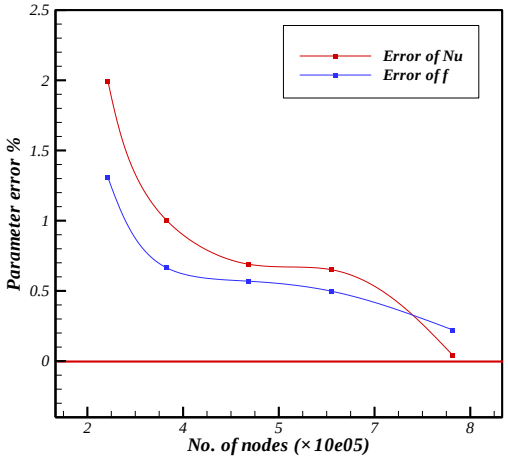

Figure 2. Grid independence test with the percentage of error.

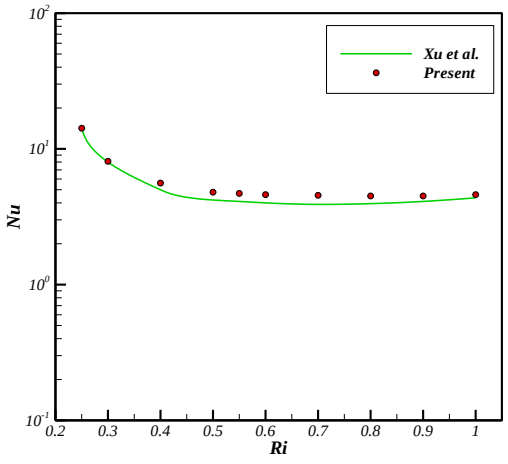

Figure 3. Validation of the average *Nu* with Xu et al. [12].

3. RESULTS AND DISCUSSION

3.1 Effect of the dimensions of the straight grooves

For the aspect ratio (*Ri* = 0.55), it is necessary to choose the highest scale for the geometric dimensions of the grooves which have a rectangular cross-section.

The result of smooth metal foam in the pipe is also graphed for comparison with the result of using the grooves in **Figure 4**, the height and width of grooves is tabulated in **Table 2.**

Table 2 Groove dimensions in mm.

(H, W)		
(6,3)	(8,3)	(10,3)
(6,4)	(8,4)	(10,4)
(6,5)	(8,5)	(10,5)

The effect of changing the width and height dimensions are measured on the value of heat transfer represented by the value of the Nusselt number and the value of the pressure drop represented by the friction factor. In addition, the values of performance are examined for each groove. Pumping power and foam volume reduction are also measured.

Effect of Reynolds Number on the Average Nusselt Number

When the two straight grooves are utilized in several geometric dimensions, the final results indicate that the Nusselt number of all cases having a groove exhibit lesser *Nu* number than the smooth metal foam pipe. Among these tested cases, the groove having dimensions of (*H6, W3*) shows the best thermal performance as shown in **Figure 4 (*a*)**. In general, as the amount of removal of metal foam increases the heat transfer rate decreases due to heat removal by conduction heat transfer. However, *Nu* number increases

with increasing the flow rate due to the force motion of molecules which leads to increase the convection heat transfer rate.

Effect of Reynolds Number on the friction factor

While the friction factor values also decrease with fewer collisions with edges of metal foam during fluid flows according to the removal of part of the metal foam. **Figure 4 (*b*)** shows that the friction factor values decrease with increasing the dimensions of the groove, and the dimension of (*H10, W5*) displays the lowest frictional losses among the others recorded is about 23%. Therefore, monotonically decreasing observed in f with *Re* in all cases.

Effect of Reynolds Number on the *PEC*

Now, to show the thermal performance and hydraulic performance simultaneously, the *PEC* is considered in this study.

Now, to show the thermal performance and hydraulic performance simultaneously, the performance evaluation criterion is considered in this study. Generally, *PEC* of all cases decreases with *Re* number, while **Figure 4 (*c*)** illustrates that the best *PEC* obtained is for (*H10, W5*). The cases having *PEC* >1 represent that the proposed designs are useful and can be adopted for further simulations and some cases *PEC*<1 in which the reduction in heat removal is greater than the decreases in friction factor which means that these proposed cases are meaningless and cannot be considered in the future studies..

Effect of Reynolds Number on the pumping power

Simultaneously, the values of the pumping power also decrease with the decrease in pressure drop. This is of great importance in conserving energy and reducing the costs. **Figure 4 (*d*)** represents the saving in pumping power with Reynolds number, it shows that the increase in the dimensions leads to increases in the value of saving pumping power.

The saving in the pumping power is denoted by

$$PPs \quad (\%) = \left|\frac{PP_{old} - PP_{new}}{PP_{old}}\right| \times 100 \qquad (24)$$

Effect of grooves on the volume reduction

There is also an important benefit of removing part of the metal foam. Making grooves in the foam could reduce the foam volume and then leads to a decrease in the weight of the solid mass and also reduce mechanization. **Table 3** shows the percentages reduction of the volume of *2SG* and different (*H*) and (*W*) in metal foam.

Table 3 Volume reduction of *2SG* and different (*H*) and (*W*) in metal foam.

H / *W*	*H6*	*H8*	*H10*
W3	3.09%	4.12%	5.22%
W4	3.97%	5.29%	6.68%
W5	4.84%	6.46%	8.14%

The volume reduction of metal foam is denoted by

$$V \quad (\%) = \left|\frac{V_{old} - V_{new}}{V_{old}}\right| \times 100 \qquad (25)$$

These cases exhibit a decrease of f, *PP* and volume reduction while a slights decrease in *Nu* is observed.

3.2 Effect of the dimensions of the helical grooves

After studying the grooves dimensions in the straight grooves, turn now to examine the effect of the two helical grooves on the performance of the system. The numbers of the pitch from one (*1P*) to four pitches (*4P*) are studied. The dimensions of the grooves considered as the height of the groove is 6 and 10 mm, while the width is kept at 5 mm.

Effect of Reynolds Number on the Average Nusselt Number

As shown in **Figure 5 (a)**, the Nusselt number increases with increasing *Re*. It can be seen that the eight grooved metal foam designs show higher *Nu* with respect to the smooth case. Among those cases, (*2P H10*) shows the superiority in heat removal particularly of higher *Re* that recorded about 5.78% compared with the smooth case. Further pitches (3 and 4) do not make a remarkable change in *Nu* and no more fluid penetrates inside the foam zone for absorbing farther heat.

Effect of Reynolds Number on the friction factor

Making helical grooves provides a desirable reduction in the friction factor in recording the greater decreasing in *f* in the cases of (*1P H10*) and (*2P H10*), which recorded about 12% compared with the smooth case. A noticeable reduction in *f* at low Re up to moderate Re, while a small reduction in *f* when *Re* > 1000 similar to that in the moody chart. There is a strong link between *f* and the thickness of the boundary layer, the boundary layer decrease with increasing *Re* and *f* is also decreased. Therefore, monotonically decreasing observed in *f* with Re, as shown in **Figure 5 (b).**

Effect of Reynolds Number on the *PEC*

The same trend of *PEC* is obtained for *2HG* with respect to *1HG* but at different levels. (*2P H10*) is still the highest hydro-thermal design among the other grooves, as shown in **Figure 5 (c)**, followed by (*3P H10*) and then (*4P H10*). In addition, the range of Re (500 < *Re* < 1250) is recorded the largest of PEC.

Effect of Reynolds Number on the pumping power

It can show that as *Re* > 500, there is no significant change in the *PPs*%. The (*1P H10*) and (*2P H10*) show the largest *PPs*% for the whole range of *Re*. A value in *PPs*% of (*1P H10*) around 18% is liable to be remarked, as shown in **Figure 5 (d)**.

Effect of grooves on the volume reduction

Another advantage of the presence of two helical grooves in the metal foam, where it leads to a decrease in volume and this leads to a decrease in the weight of the system and reduces operating costs as well. **Table 4** shows the relationship between the number of pitch and the percentage of metal removal.

Table 4 The percentages of volume reduction of *2HG*.

(H,W) / *P*	*(H6,W5)*	*(H10,W5)*
1P	4.56%	7.89%
2P	4.81%	8.29%
3P	5.20%	8.90%
4P	5.69%	9.71%

The velocity vectors and the isothermal contours of the flow through the pipe without and with *2SG* along the pipe are shown in **Figure 6 (*a*) – (*c*),** for (*2SG*) and (*H10, W5*) and (*2HG 2P*) with (*H10, W5*), *Re* = 1000 and *Ri* = 0.55. The higher fluid velocity is monitored with smoothed foam pipe due to the smaller cross-sectional area of the clear fluid zone. Moreover, grooved foam pipe i.e., (b) thinner hydraulic boundary layer due to a smaller amount of foam used. In that case, lower heat removal by conduction leads to lower fluid temperature for same *Re* and consequently smaller heat removal by grooved ones. It also can be seen that the fluid is penetrated deeply in

the foam metal in the case of *2HG* more than the smooth one due to secondary water flow as shown in **Figure 6 (*c*)**. More fluid penetrations could cause a thinner boundary layer and then higher heat transfer. Thus, *2HG* could reduce the pumping power required to simultaneously increase the heat removal.

Thus, several advantages can be extended as; improvement of heat transfer rate, less pressure drop for given flow rates, high thermal and hydraulic performance, lower pumping power, cost saving on the total life-cycle basis, improving plant run length, remove the part of the metal and lighter in weight.

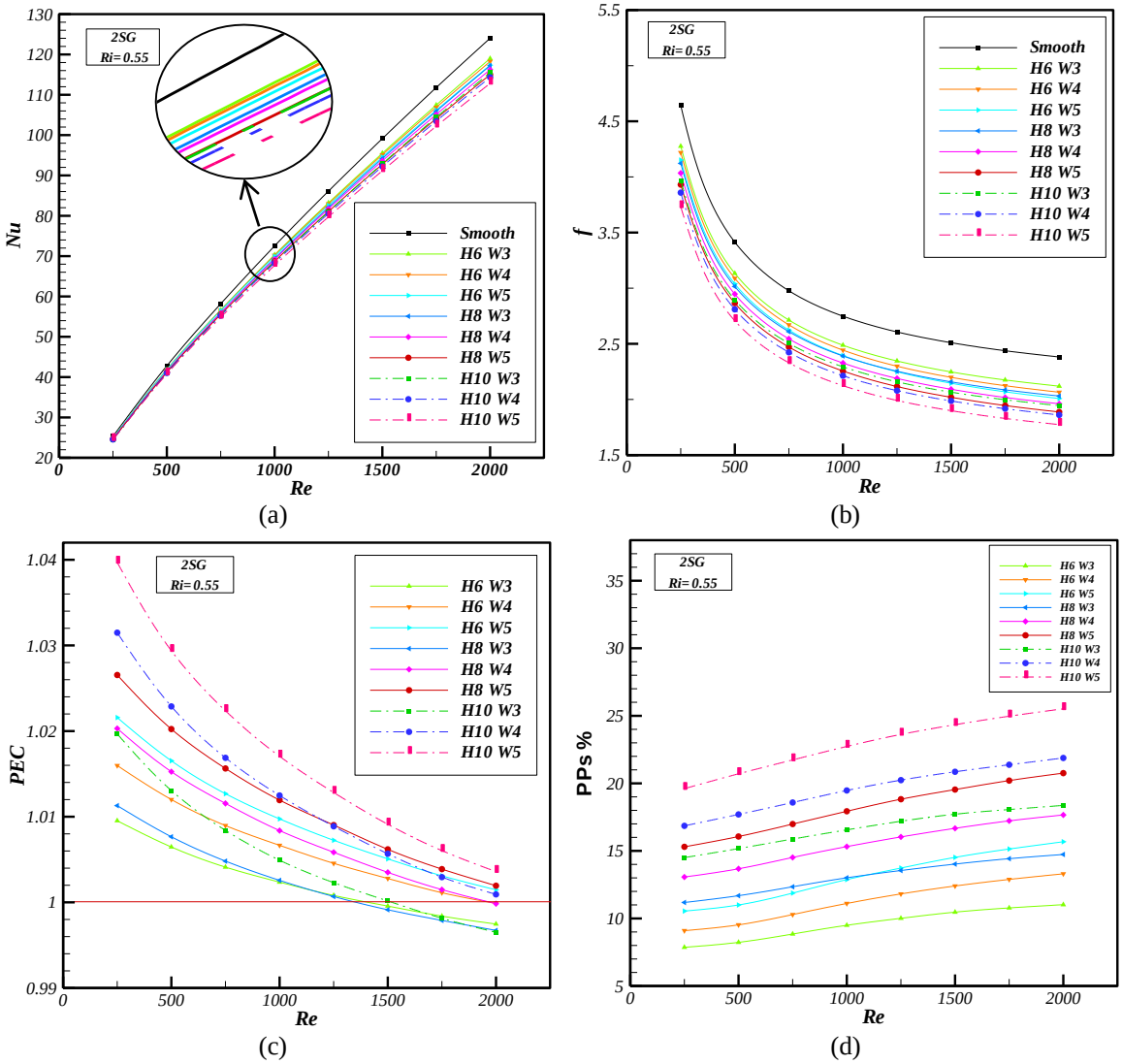

Figure 4. Effect of the groove dimensions (*H, W*) on (a) Nusselt number, (b) friction factor, (c) *PEC* and (d) *PPs*% for two straight grooves (*2SG*) and *Ri*=0.55.

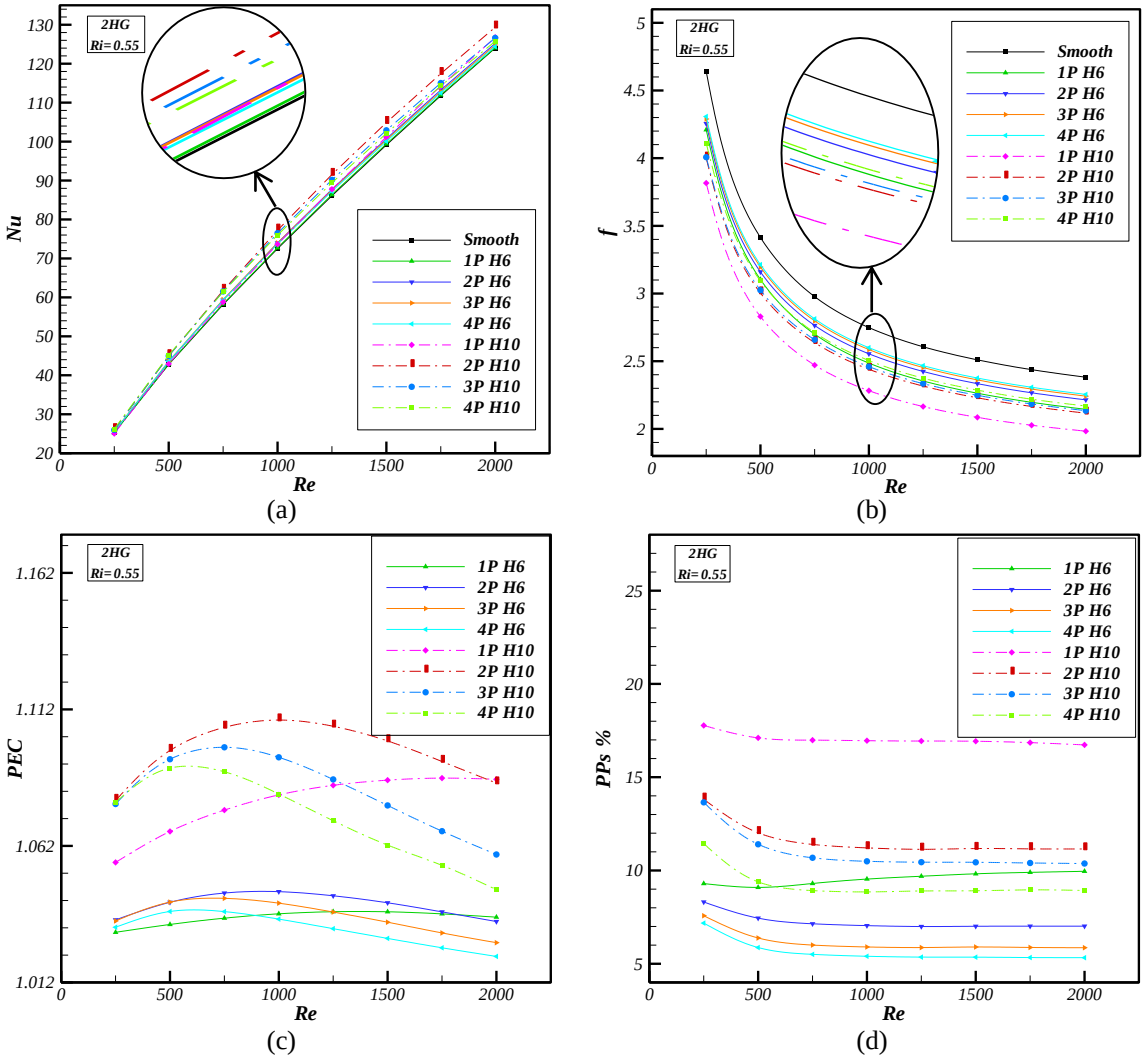

Figure 5. Effect of pitch number of two helical grooves on the (a) Nusselt number, (b) friction factor, (c) *PEC* and (d) *PPs*% at *Ri* = 0.55.

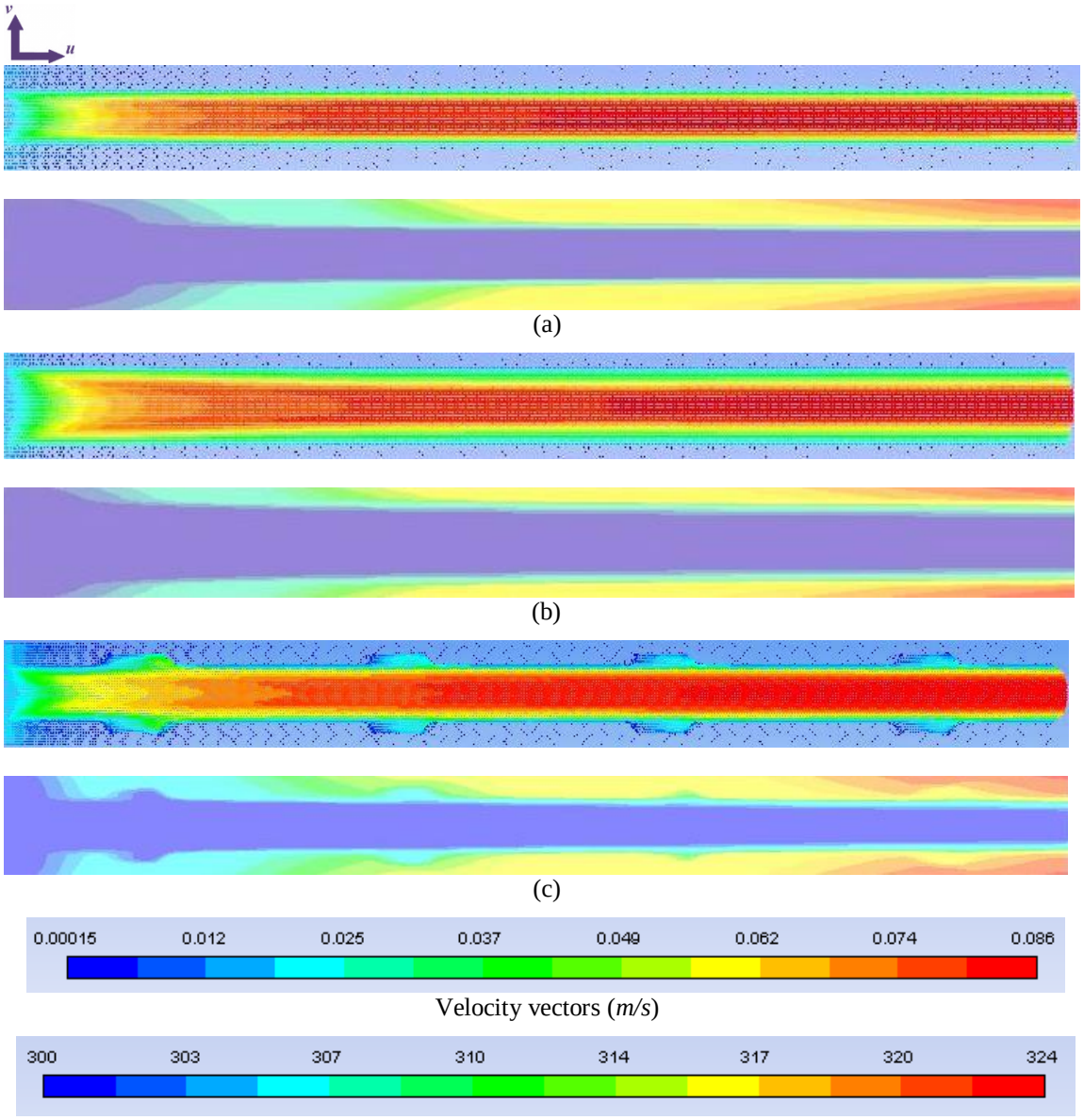

Figure 6 Vectors of velocity and isotherm contours at *Ri*=0.55 and *Re*=1000 for (a) smooth case, (b) *2SG* with (*H10, W5*), and (c) *2HG* and 2*P* with (*H10, W5*).

Conclusions

Numerical solution is implemented to study the heat transfer and fluid flow in a pipe partially filled with grooved metallic foam with non-Darcy laminar forced convection. The current paper studies the effects of nine different dimensions of rectangular grooves over a wide range for Reynolds number ($250 \leq Re \leq 2000$). A new design of metallic foam is proposed in order to enhance the hydrothermal performance of such heat exchangers as pipes. Through the performance evaluation, the best values obtained when (*H, W*) equals to (10, 5) mm. The grooves in the metal foam play an important role in term of reducing the pumping power up to 23%, in addition to removing part of the metal, which leads to a decline in the weight of the system

8.14%, with a slight decrease in the Nusselt number (–6%). The results shows that for the helical groove, the (*2HG 2P*) and (*H10, W5*) increase the Nusselt number nearly 5.23% and decrease the pumping power around 19%. The amount of material decreased 7.15% and the *PEC* is around 1.11 at the *Re* = 1000.

Nomenclature

Meaning	Symbol	Units
Area	A	m^2
cross-sectional area	A_c	m^2
inertia coefficient	C_F	m^{-1}
Computational fluid dynamic	CFD	
specific heat	c_p	$J\ kg^{-1}\ K^{-1}$
pipe diameter	D	m
Metal foam diameter	d	m
Friction factor	f	
Height	H	m
Convection heat transfer coefficient	h	$Wm^{-2}\ K^{-1}$
permeability	K	m^2
thermal conductivity	k	$W\ m^{-1}\ K^{-1}$
Effective thermal conductivity	k_e	$W\ m^{-1}\ K^{-1}$
length	L	m
Nusselt number	Nu	
volumetric flow rate	$\bar{Q}$	$m^3\ s^{-1}$
performance evaluation criterion	PEC	
pumping power	PP	W
saving pumping power	PPs	%
wall heat flux	q''	$W\ m^{-2}$
Reynolds number	Re	
Dimensionless diameter ratio, Ri=d/D	Ri	
temperature	T	K
axial velocity	u	$m\ s^{-1}$
Volume	V	m^3
volume reduction	Vr	%
Width	W	m
pressure drop	ΔP	$N\ m^{-2}$
Greek symbols		
dynamic viscosity of the fluid	μ	$N\ s\ m^{-2}$
Thermal diffusivity	α	$m^2\ s^{-1}$
porosity	ε	
fluid density	ρ	$kg\ m^{-3}$
Subscripts		
effective	e	
fluid	f	
grooved case	new	
smooth case	old	

References

[1] X. Chen, F. Tavakkoli, and K. Vafai, "Analysis and characterization of metal foam-filled double-pipe heat exchangers", Numerical Heat Transfer, Part A : Applications : An International Journal of Computation and Methodology 68 (2015) 1031–1049.

[2] V. V. Calmidi and R. L. Mahajan, "Forced convection in high porosity metal foams", Journal of Heat Transfer, 122 (2000) 557–565.

[3] M. Dehghan, M. S. Valipour, and S. Saedodin, "Temperature-dependent conductivity in forced convection of heat exchangers filled with porous media : A perturbation solution", Energy Conversion and Management, 91 (2015) 259–266.

[4] M. Mahdavi, M. Saffar-Avval, S. Tiari, and Z. Mansoori, "Entropy generation and heat transfer numerical analysis in pipes partially filled with porous medium", International Journal of Heat and Mass Transfer, 79 (2014) 496–506.

[5] M. A. Teamah, W. M. El-maghlany, and M. M. Khairat, "Numerical simulation of laminar forced convection in horizontal pipe partially or completely

filled with porous material", International Journal of Thermal Sciences, 50 (2011) 1512–1522.
[6] P. Taylor, M. Maerefat, S. Y. Mahmoudi, and K. Mazaheri, "Numerical Simulation of Forced Convection Enhancement in a Pipe by Porous Inserts", Heat Transfer Engineering, 32 (2011) 45-56.
[7] D. Poulikakos and M. Kazmierczak, "Forced convection in a duct partially filled with a porous material", Journal of Heat Transfer, 109 (1987) 653–662.
[8] W. Lu, C. Y. Zhao, and S. A. Tassou, "Thermal analysis on metal-foam filled heat exchangers. Part I: Metal-foam filled pipes", International Journal of Heat and Mass Transfer, 49 (2006) 2751–2761.
[9] S. Mancin, C. Zilio, A. Diani, and L. Rossetto, "Experimental air heat transfer and pressure drop through copper foams", Experimental Thermal and Fluid Science, 36 (2012) 224–232.
[11] Z. Qu, H. Xu, and W. Tao, "Numerical Simulation of Non-Equilibrium Conjugate Heat Transfer in Tubes Partially Filled with Metallic Foams", Journal of Thermal Science and Technology, 7 (2012) 151–165.
[12] H. J. Xu, Z. G. Qu, and W. Q. Tao, "Analytical solution of forced convective heat transfer in tubes partially filled with metallic foam using the two-equation model", International Journal of Heat and Mass Transfer, 54 (2011) 3846–3855.
[13] A. A. Sertkaya, K. Altınısık, and K. Dincer, "Experimental investigation of thermal performance of aluminum finned heat exchangers and open-cell aluminum foam heat exchangers", Experimental Thermal and Fluid Science, 36 (2012) 86–92.
[14] C. Yang, A. Nakayama, and W. Liu, "Heat transfer performance assessment for forced convection in a tube partially filled with a porous medium", International Journal of Thermal Sciences, 54 (2012) 98–108.
[15] Z. G. Qu and W. Q. Tao, "Thermal modeling of forced convection in a parallel-plate channel partially filled with metallic foams", Journal of Heat Transfer, 133 (2011) 20–22.
[16] D.A. Nield and A. Bejan, "Convection in Porous Media", 3rd Edition, Springer, New York, (2006).
[17] T. D. Canonsburg, "ANSYS Fluent User's Guide", vol. 15317, (2017).
[18] F. P. Incropera, D. P. DeWitt, T. L. Bergman and A. S. Lavine, "Fundamentals of Heat and Mass Transfer", 7th Edition, John Wiley and Sons, U.S.A., (2011).
[19] R. A. Mahdi, H. A. Mohammed, and K. M. Munisamy, "The effect of various open cell aluminium foam geometrical shapes on combined convection heat transfer with nanofluid", International Journal of Emerging Technology and Advanced Engineering, 3 (2013) 615–629.